CHAPTER IV

RESULTS AND DISCUSSION

4.1 Influence of current of arc discharge using C-C electrodes

In this work, first arc discharge in liquid nitrogen was carried out by using carbon electrodes. As explained in chapter 3 the cathode was carbon rod with diameter of 20mm while carbon rod with diameter of 6mm was employed as anode to make sure that contact between both electrode could be obtained during arc operation. It was clearly observed that stable arc could be achieved even though the applied current was just 50A. With an increase in arcing current, arcing could be operated more stably. In each experiment, arcing was normally operated for 3-5 minutes. After arcing, both sedimentary and deposit cathode products could be obtained. Then they were taken to characterize by various analytical instruments. The effect of arcing current on their characterishes would be explained in the following section.

4.1.1 Microscopic analyses of the obtained products

After the arc discharge, two types of products, cathode deposit and sedimentary particles could be observed. Generally, no anode deposit could be observed from arc discharge in liquid nitrogen. Also, there are no floating particles obtained from arc discharge in carbon-carbon electrodes.

Microscopic analyses shown in Figure 4.1-4.2 reveal that sedimentary obtained from arcing current of 20-160A in liquid nitrogen are CNHs with nominal diameter of 50-150 nm, MW-CNTs with nominal diameter of 8-25 nm and length of 150-250 nm, and multi-shelled carbon nanoparticles with diameters of 30-60 nm. These mixed products were seen everywhere by scanning observations, indicating that the purity of

CNPs is very high. With an increase in arc current fraction of carbon nanoparticles become drastically decreased. Within the synthesize product, fraction of CNHs and multi-shelled carbon nanoparticles became higher but that of MW-CNTs became decreased.

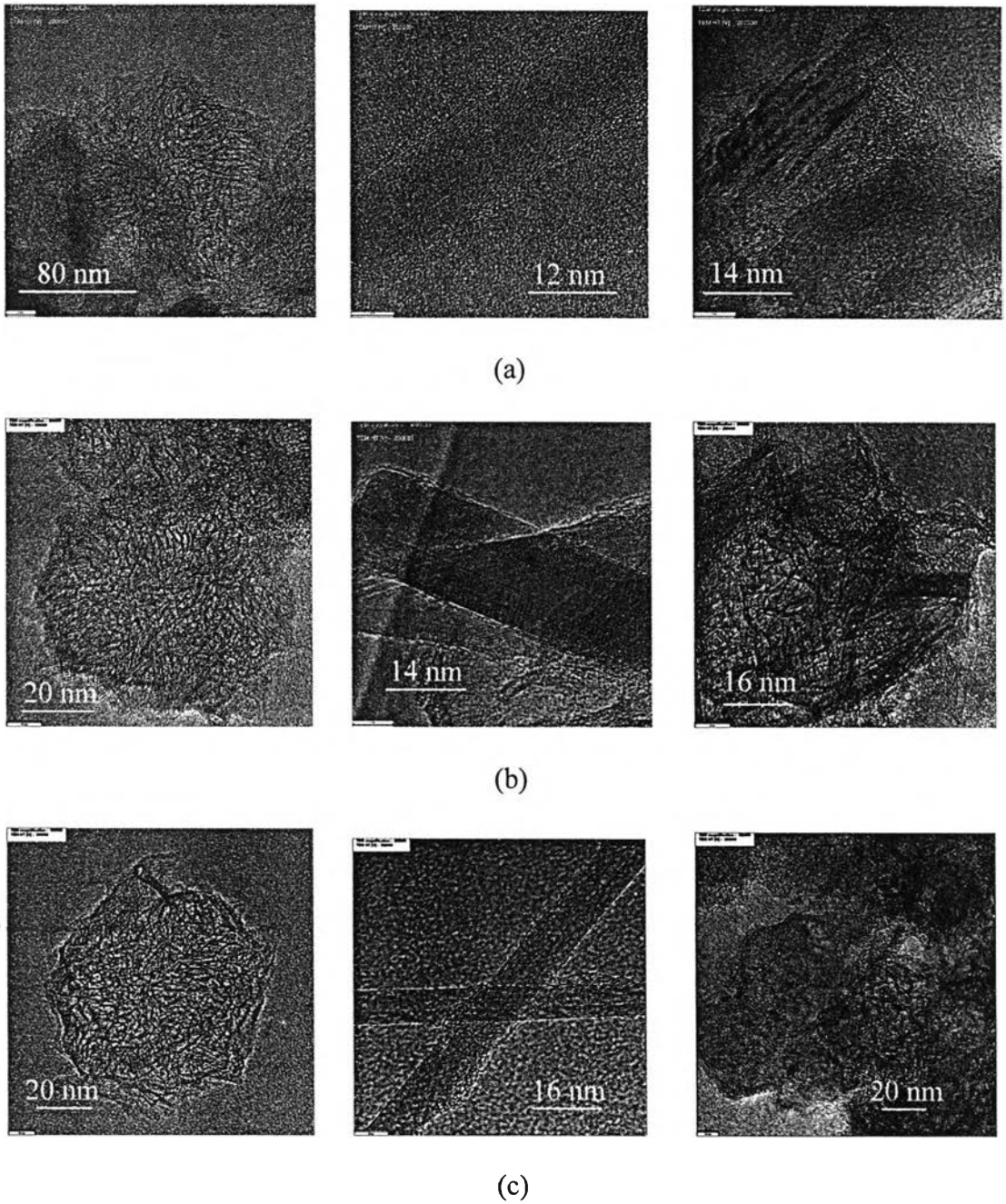

Figure 4.1 TEM images from arcing in liquid nitrogen of sedimentary particles, (a) arcing current range 50A, (b) arcing current range 75A, and (c) arcing current

range 100A which mainly consists of CNHs, MW-CNTs and multi-shelled CNPs respectively.

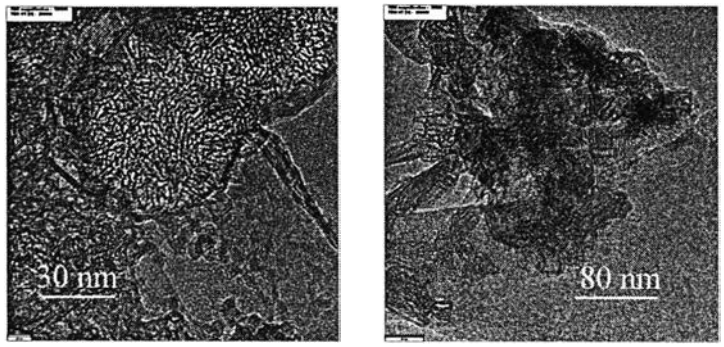

(d)

Figure 4.2 TEM images from arcing in liquid nitrogen of sedimentary particles, (d) arcing current range 125A which mainly consists of CNHs, and multi-shelled CNPs respectively.

Microscopic analyses shown in Figure 4.3-4.4 reveal that cathode deposit obtained from arcing current of 50-125A in liquid nitrogen are MW-CNTs with nominal diameter of 8-15 nm and length of 150-250 nm, and multi-shelled carbon nanoparticles with diameters of 40-160 nm. These mixed products were seen everywhere by scanning observations, indicating that the purity of CNPs is very high. The increasing arc current had fraction of carbon nanoparticles become drastically decreased carbon nanoparticles could be generated increase multi-shelled carbon nanoparticles and then decrease MW-CNTs.

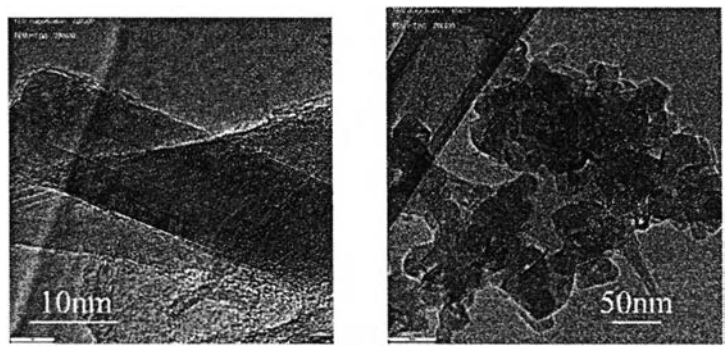

(a)

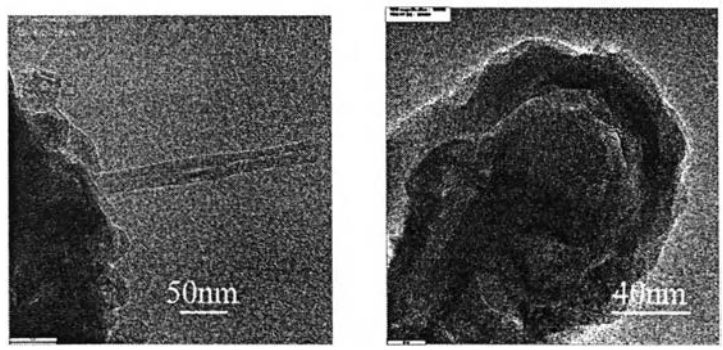

(b)

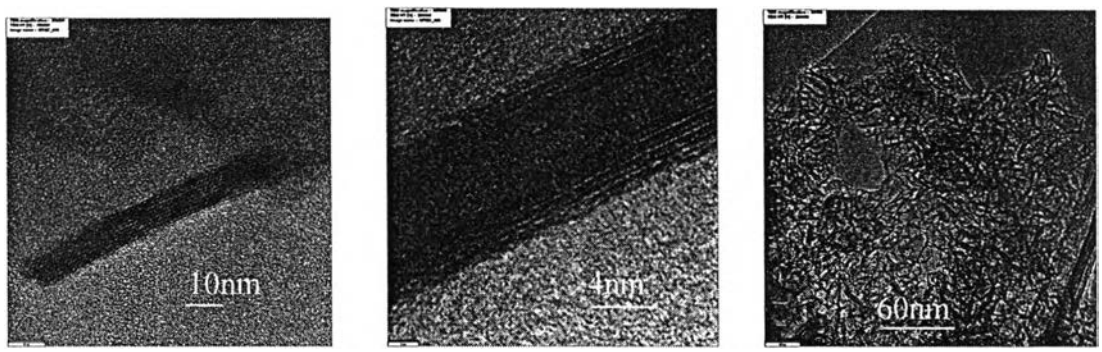

(c)

Figure 4.3 TEM images from arcing in liquid nitrogen of cathode deposit particles, (a) arcing current range 50A, (b) arcing current range 75A, and (c) arcing current range 100A which mainly consists of MW-CNTs and multi-shelled CNPs respectively.

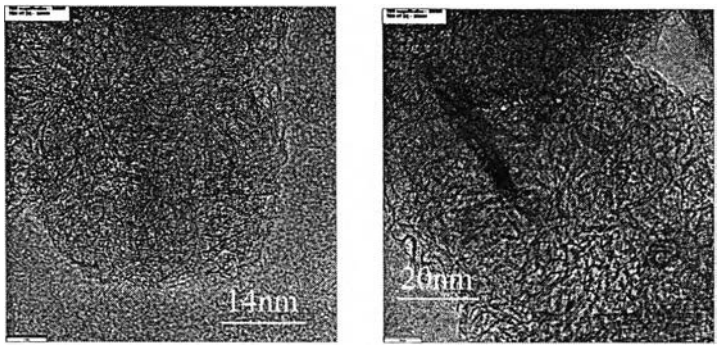

(d)

Figure 4.4 TEM images from arcing in liquid nitrogen of sedimentary particles, (d) arcing current range 125A which mainly consists of multi-shelled CNPs.

4.1.2 The yield of carbon nanoparticles

The yield of CNPs was determined from ratio of weight of as-received product to that of consumed anode. The yields of the products shown in Figure 4.5 are strongly dependent on the arcing current. In every experiment using carbon-carbon electrodes, only anode is consumed but on cathode there are some deposits, leading to weight gain. Therefore, this result implies that graphite anode could play a role as the carbon source for producing CNPs. In contrast, for 'arc in liquid nitrogen' system, carbon atoms are supplied only from the graphite anode electrodes, resulting in the highest production yield which is approximately 91%.

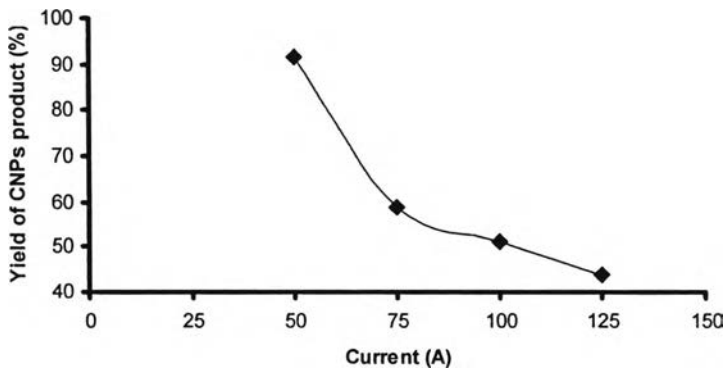

Figure 4.5 The yields of C-C electrodes, anode ID 6mm liquid nitrogen

The formation rate of cathode deposit slightly decreases as current discharge and graphite anode vaporization are increased that graphite anode evaporates rapidly, thus carbon atom losses with liquid nitrogen.

4.1.3 Particle size distribution

Typical average particle sizes of the CNPs evaluated by DLS are shown in Figure 4.6-4.7. It is known that particle size distribution of the obtained product is typically log-normal. For the C_2H_5OH systems, the mean hydrodynamic diameter of CNPs lies in a range of 270-340nm. Based on this result, it could be implied that the selectivity of elongated-structures in C_2H_5OH is higher than in H_2O, because the concentration of carbon atoms in C_2H_5OH system is much higher than in H_2O, leading to the enhanced growth of elongated particles which need more carbon-supply.

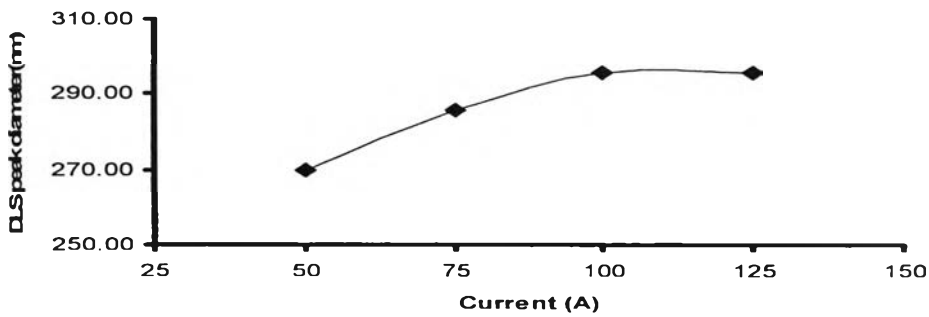

Figure 4.6 The particle size distribution of c-c electrodes of cathode deposit particles

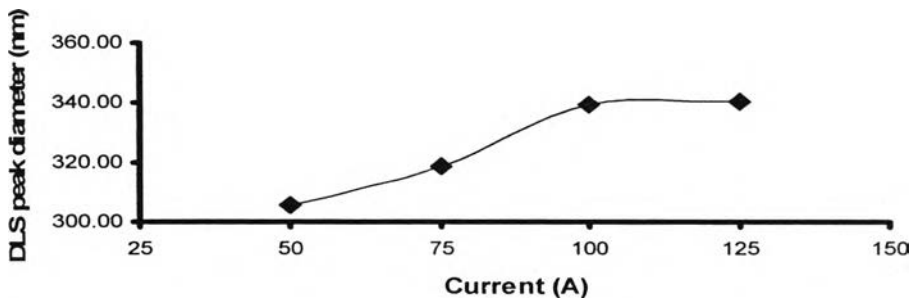

Figure 4.7 The particle size distribution of c-c electrodes of sedimentary particles

4.1.4 Raman Spectroscopic analysis

The ratio of the intensity of graphitic band (G-band, 1580 cm^{-1}) to that of disorder band (D-band, 1353 cm^{-1}) in the Raman spectra of CNPs containing deposits are shown in Figure 4.8-4.9. With an increase in current discharge range 50-125A, the G/D ratio of the obtained CNPs deviates within a range of 1.54 to 2.4. The G/D ratio becomes highest when current discharge 50A is used and becomes lowest when current discharge 125A is employed. On the other hand, for the cases of arc discharge using carbon anode of 6mm, the G/D ratio is significantly decreased with the increasing arc current because of at higher arc current generates decreasing the structure of carbon nanotutes obtained.

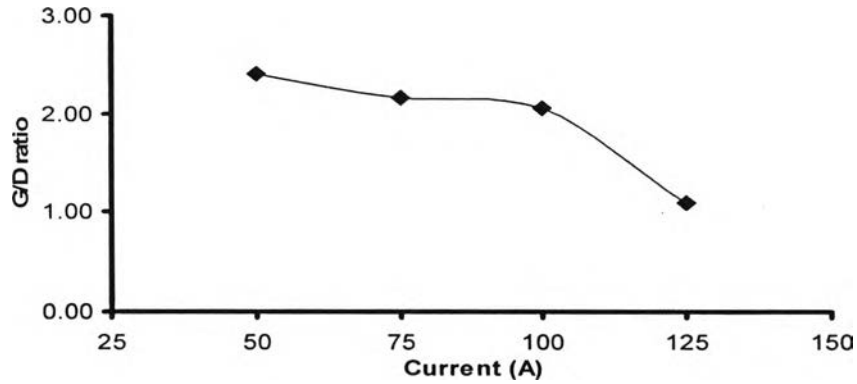

Figure 4.8 G/D ratio of c-c electrodes of cathode deposit particles

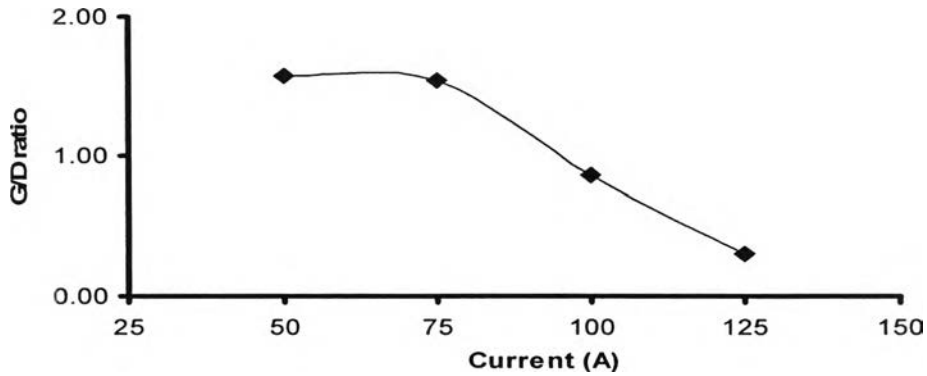

Figure 4.9 G/D ratio of c-c electrodes of sedimentary particles

4.2 Influence of current of arc discharge using Fe-C electrodes

The experimental result could be obtained under the condition of arcing with an increase in arcing current in a range of 100-250A in liquid nitrogen. Arc discharge was carried out by using carbon and iron electrodes. As explained in chapter 3 the cathode was iron rod with diameter of 20mm while carbon rod with diameter of 3-6mm was employed as anode to make sure that contact between both electrode could be obtained during arc operation. It was clearly observed that stable arc could be achieved even though the applied current was just 100A. In each experiment, arcing was normally operated for 3-5 minutes. After arcing, sedimentary products could be obtained. Then they were taken to characterize by various analytical instruments. The effect of arcing current on their characterishes would be explained in the following section.

4.2.1 Microscopic analyses of the obtained products

After the arc discharge using Fe-C electrodes submerged in liquid nitrogen, only sedimentary products could be observed. Generally, no anode deposit could be observed from arc discharge in liquid nitrogen. Also, there are no floating particles and no cathode deposit obtained from these experiments.

Microscopic analyses shown in Figure 4.10-4.11 reveal that sedimentary obtained from using arc current of 100-250A with 3mm anode products are CNCs with nominal diameter of 50-400 nm and multi-shelled carbon nanoparticles with diameters of 50-350 nm. These as-received products were seen everywhere by scanning observations, indicating that the purity of CNCs is very high. With an increase in arc current fraction of Fe-encapsulated carbon nanocapsules become

higher while the fraction of multi-shelled carbon nanoparticles without Fe become drastically decreased.

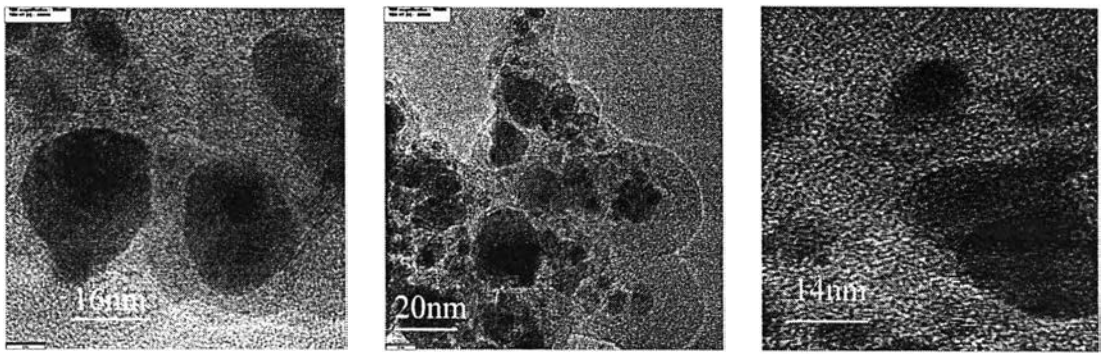

(a) (b)

Figure 4.10 TEM images from arcing in liquid nitrogen of sedimentary particles, (a) arcing current range 100A and (b) arcing current range 125A which mainly consists of agglomeration Fe coated by carbon and CNCs respectively.

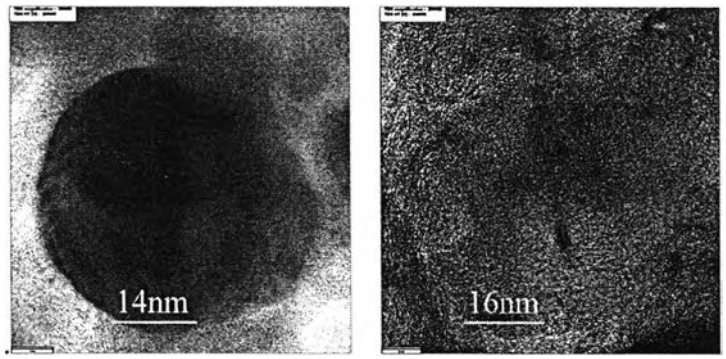

(c)

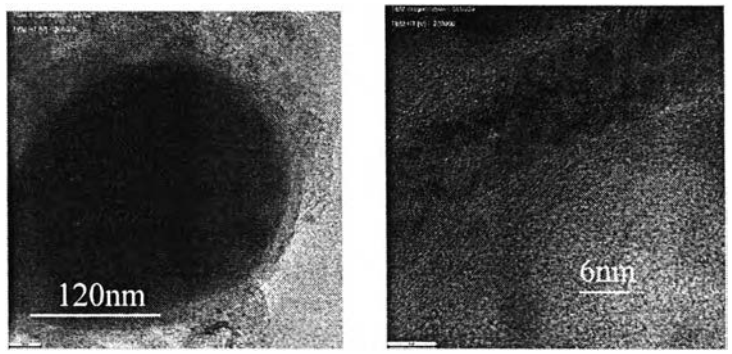

(d)

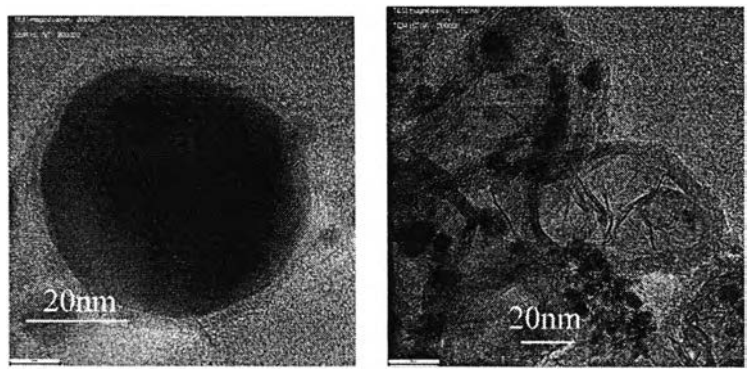

(e)

Figure 4.11 TEM images from arcing in liquid nitrogen of cathode deposit particles, (c) arcing current range 150A, (d) arcing current range 175A, and (e) arcing current range 200A which mainly consists of CNCs and multi-shelled CNPs respectively.

When a bigger carbon anode electrode with ID of 6mm was employed the as-received products were also similar to carbon anode electrode with ID of 3mm. Microscopic analyses shown in Figure 4.12 reveal that sedimentary obtained from arcing current of 175-250A in liquid nitrogen by using anode with diameter of 6mm which are CNCs with nominal diameter of 40-210 nm and multi-shelled carbon nanoparticles with diameters of 50-250 nm. These mixed products were seen everywhere by scanning observations, indicating that the high purity of CNCs could be obtained when the employed arc current is equal to or larger than 175A.

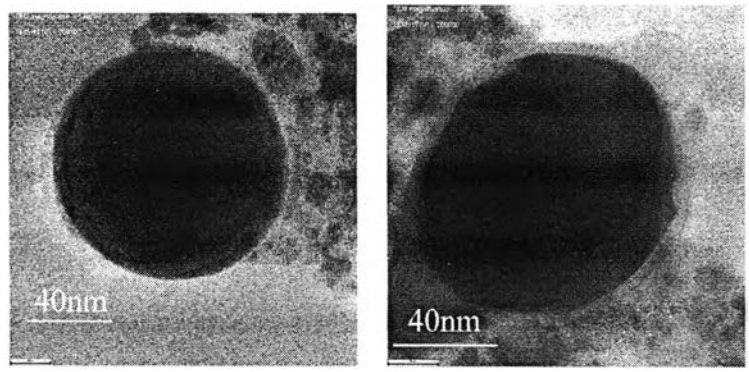

(a) (b)

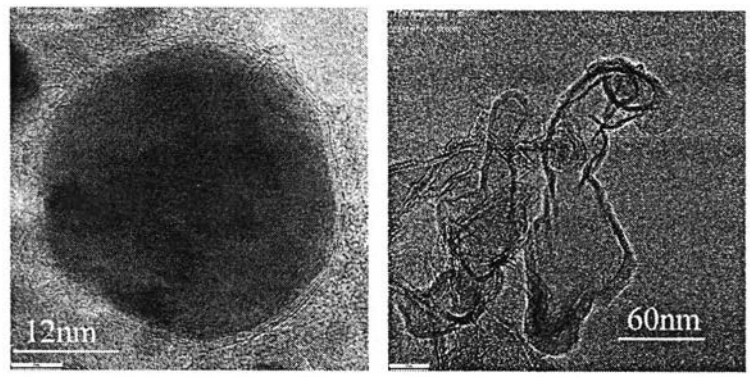

(c)

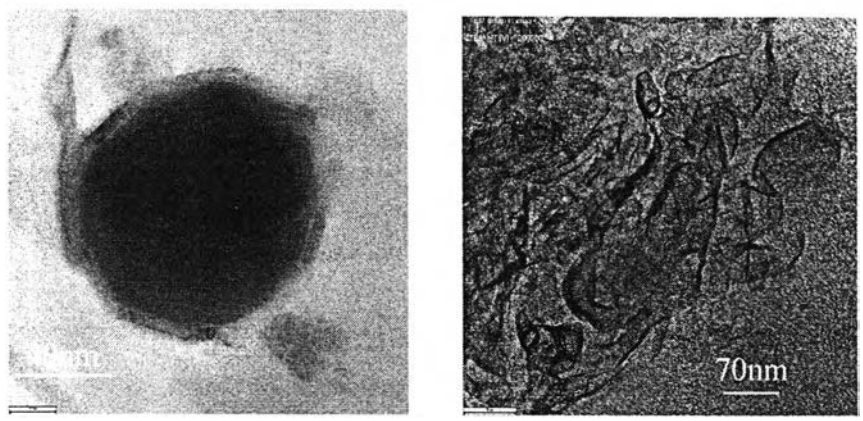

(d)

Figure 4.12 TEM images from arcing in liquid nitrogen of sedimentary particles, (a) arcing current range 175A and (b) arcing current range 200A which mainly consists of CNCs only and then (c) arcing current range 225A and (d) arcing current range 250A which mainly consists of CNCs and multi-shelled CNPs respectively.

4.2.2 The yield of carbon nanoparticles

The yield of CNPs was determined from ratio of weight of as-received product to that of consumed anode. The yields of the products shown in Figure 4.13-4.14 are dependent on the arcing current. . In every experiment using iron-carbon electrodes, anode and cathode are consumed but on cathode there are some deposits, leading to weight gain. Therefore, this result implies that graphite anode, and iron cathode could play a role as the carbon source, and iron source for producing CNCs, and CNPs. In contrast, for 'arc in liquid nitrogen' system, carbon atoms are supplied only from the graphite anode electrodes, resulting in the highest production yield which is approximately 80%.

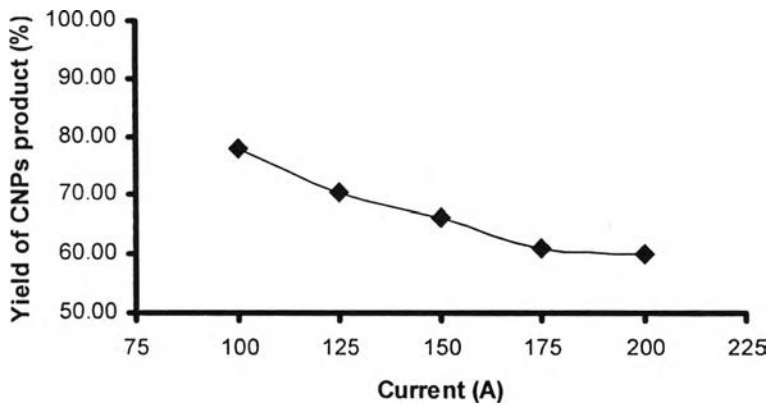

Figure 4.13 The yields of Fe-C electrodes, anode ID 3mm liquid nitrogen

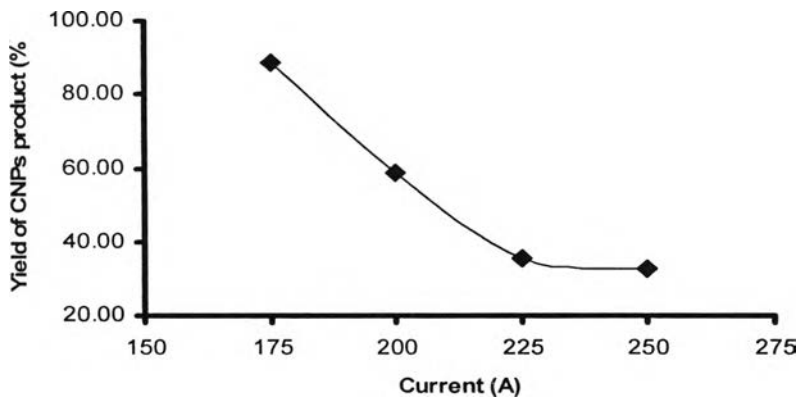

Figure 4.14 The yields of Fe-C electrodes, anode ID 6mm liquid nitrogen

The formation rate of sedimentary slightly decreases as current discharge, iron cathode vaporization and graphite anode vaporization are increased that graphite, and iron electrodes evaporate rapidly, thus carbon atom losses with liquid nitrogen and iron cathode rod is melted rapidly until it cannot growth with carbon atom.

4.2.3 Particle size distribution

Typical average particle sizes of the CNPs evaluated by DLS are shown in Figure 4.15-4.16. It is known that particle size distribution of the obtained product is typically log-normal. For the C_2H_5OH systems, the mean hydrodynamic diameter of CNPs lies in a range of 140-360nm. Based on this result, it likes 4.1.3 case c-c electrodes, leading to the enhanced growth of elongated particles which need more carbon-supply.

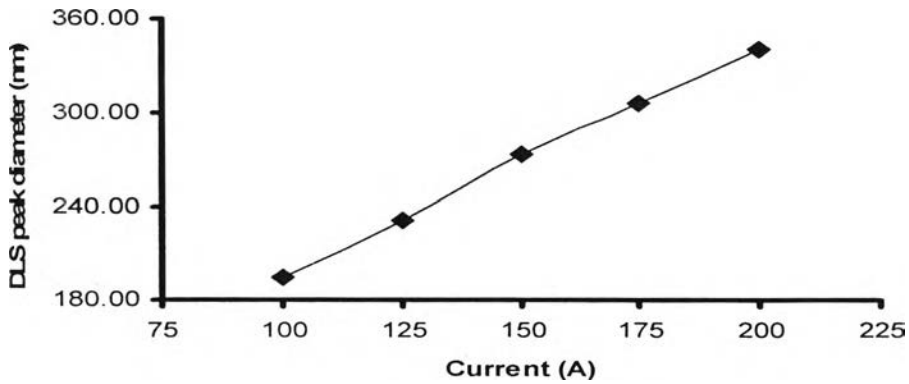

Figure 4.15 The particle size distribution of fe-c electrodes of anode ID 3mm

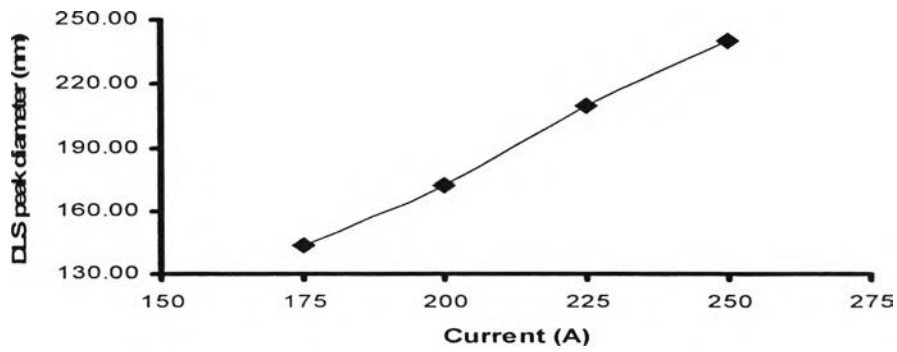

Figure 4.16 The particle size distribution of fe-c electrodes of anode ID 6mm

4.2.4 Raman Spectroscopic analysis

The ratio of the intensity of graphitic band (G-band, 1580 cm^{-1}) to that of disorder band (D-band, 1353 cm^{-1}) in the Raman spectra of CNPs containing deposits are shown in Figure 4.17-4.18. With an increase in current discharge range 100-250A, the G/D ratio of the obtained CNPs deviates within a range of 0.55 to 1.84. The G/D ratio becomes optimal when current discharge of 225A is used then it decreased with a function increase of arc current to 250A. On the other hand, for the cases of arc discharge using smaller carbon anode of 3 mm, the G/D ratio is significantly increased with the increasing arc current because of the formation of products is generated form the increasing crystallization of carbon nanocapsules.

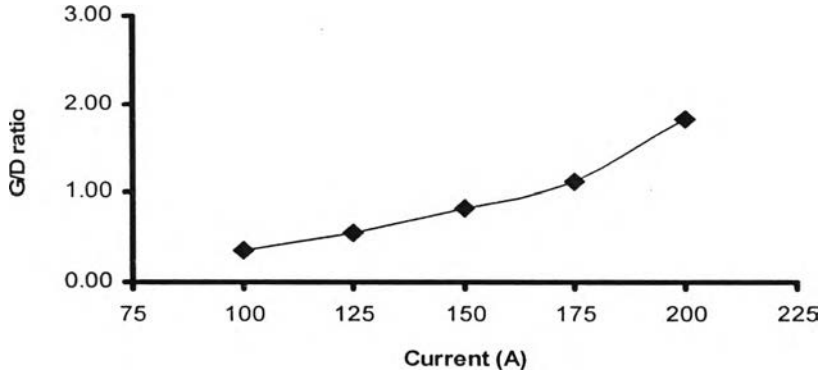

Figure 4.17 G/D ratio of synthesized product with 3mm anode

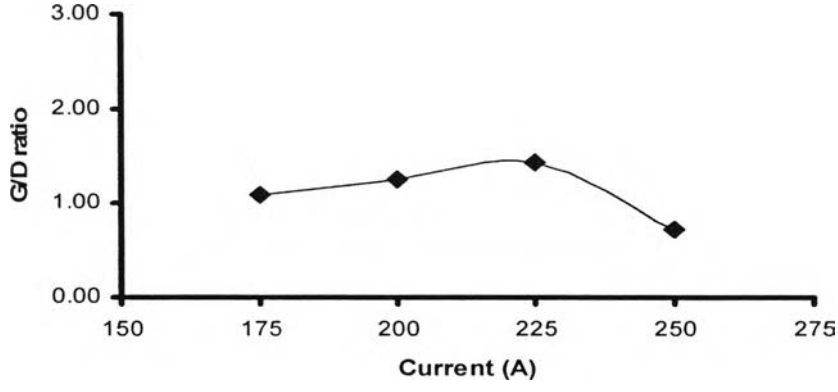

Figure 4.18 G/D ratio of synthesized product with 6mm anode

4.2 Influence of concentration of CNPs on polypropylene (PP)

Using differential Scanning Calorimetric analyses

The PP nanocomposites were prepared using the melt mixing process. The samples obtained were tested using DSC. It revealed that presence of modified carbon nanoparticles (CNPs) in PP resulted in a shift of the onset and peak temperatures towards lower values. Thermo mechanical analysis (TMA) was also used to monitor the changes in volume expansion of PP in the presence of CNPs sheets.

The crystallization peaks recorded during crystallization of i-PP blended with CNPs (5, 10 and 15%weight i-PP), are shown in Figure 4.19. The PP nanocomposite with 5wt% of CNPs exhibited the similar crystallinity as seen in the pure i-PP. However, the PP nanocomposites with 10 and 15wt% of CNPs showed the lower crystallinity than that of the pure i-PP. During crystallization, the increasing CNPs content compounded with i-PP exhibits a decrease in capability of nucleation CNPs.

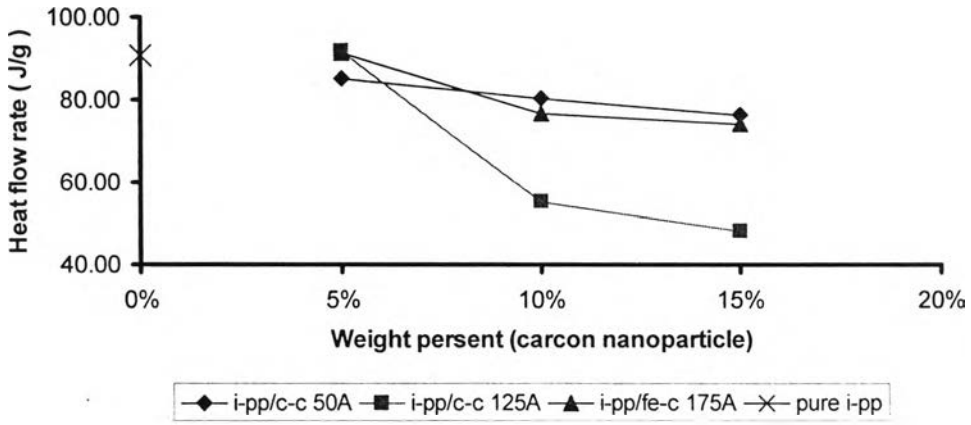

Figure 4.19 DSC peaks recorded crystallization for i-PP blended with CNPs (5, 10 and 15%weight i-PP).

Based on the crystallization peaks, the melting temperature (T_m) can be measured. The T_m values are plotted in Figure 4.20 as a function of CNPs concentration. For all samples, increased concentrations of CNPs apparently resulted in lower T_m. It was suggested that addition of 5, 10 and 15% of CNPs in i-PP rendered lower crystallinity of the PP nanocomposites obtained.

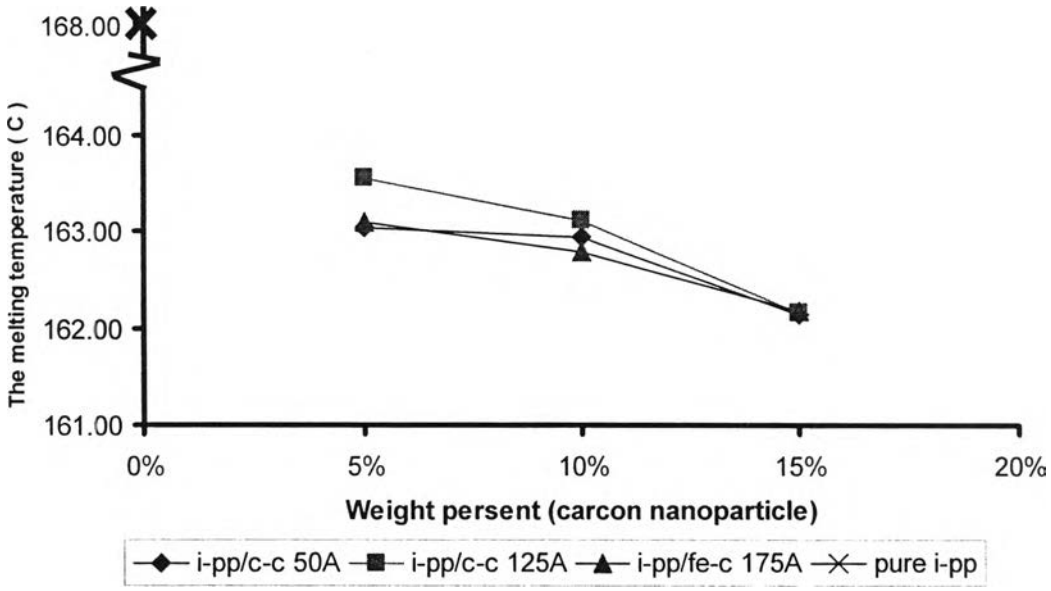

Figure 4.20 The peak melting temperature (T_m) for i-PP/CNPs nanocomposites, as a function of concentrations CNPs.